Superconductivity and magnetism of $Sm_{1.85-x}Gd_xCe_{0.15}CuO_{4-\delta}$ and $Gd_{2-y}Ce_yCuO_{4-\delta}$ crystals

Y. Nagata,[1,*] T. Shioga,[1] T. Taniguchi,[1] T. Uchida,[2] L. Zhang,[3] M. D. Lan,[4] and H. Samata[5]
[1]*College of Science and Engineering, Aoyama Gakuin University Chitosedai, Setagaya, Tokyo 157-8572, Japan*
[2]*Tokyo Institute of Polytechnics, Iiyama, Atsugi, Kanagawa 243-0297, Japan*
[3]*Department of Physics and Geology, California State University, Stanislaus, 801 West Monte Vista, Turlock, California 95382*
[4]*Department of Physics, National Chung Hsing University, Taichung 402, Taiwan, Republic of China*
[5]*Faculty of Mercantile Marine Science, Kobe University of Mercantile Marine Fukaeminami, Higashinada, Kobe 658-0022, Japan*
(Received 5 June 2001; revised manuscript received 5 September 2001; published 12 February 2002)

The magnetism and superconductivity of $Sm_{1.85-x}Gd_xCe_{0.15}CuO_{4-\delta}$ and $Gd_{2-y}Ce_yCuO_{4-\delta}$ crystals were investigated. In the $Sm_{1.85-x}Gd_xCe_{0.15}CuO_{4-\delta}$ system, superconductivity is suppressed by Gd substitution, and temperature-induced magnetic transitions appear at 3, 7, and 135 K above $x=1.2$ Cu spins have an antiferromagnetic (AF) order along the [110] direction among these transitions, and a weak-ferromagnetic (WF) moment due to a canting of Cu spins appears along the $[\bar{1}10]$ direction at $T\leqslant 3$ K and 7 K$\leqslant T\leqslant$135 K. The AF order at 3 K$\leqslant T\leqslant$7 K changes into a canted spin configuration via field-induced spin reorientation and induces the WF moment. The Néel temperature T_{NCu} (135 K at $x=1.2$) and spin-reorientation temperature T_{SR} (7 K at $x=1.2$), which are due to the Cu sublattice and are observed at low field intensity, increase with increasing x. Sm spins have an antiferromagnetic order along the [001] direction at $x=0$ below the Néel temperature T_{NR} ($\sim$5 K), but T_{NR}, which is observed for low x at high field intensity, decreases with increasing x and disappears at $x\approx 1$. Gd spins have an antiferromagnetic order along the $[\bar{1}10]$ direction for specimens with $x>1.4$ near 3 K. The change in the geometry of rare-earth and Cu spins resulting from Gd substitution is considered to be the reason for the suppression of superconductivity.

DOI: 10.1103/PhysRevB.65.104506 PACS number(s): 74.72.Jt, 74.25.Ha, 75.30.Kz

I. INTRODUCTION

The discovery of superconductivity in $R_{2-y}Ce_yCuO_{4-\delta}$ (R=Pr, Nd, Sm, or Eu) systems aroused considerable attention since these were the only copper oxide systems showing electron-type superconductivity.[1] The parent insulating compound R_2CuO_4 crystallizes in a tetragonal structure (T' phase) in which the copper ions are surrounded by a square planar arrangement of oxygen ions. The existence of an antiferromagnetic order in the Cu sublattice has been revealed for R_2CuO_4 (R=Pr, Nd, Sm, or Gd) by neutron diffraction.[2–12] The antiferromagnetic order of Cu spins in the CuO_2 plane occurs at a temperature between 200 and 300 K. When R^{3+} is replaced with Ce^{4+}, negative carriers are injected into the CuO_2 plane to compensate the valence of rare-earth sites, and the antiferromagnetic order disappears in accordance with the carrier doping; in addition, superconductivity with a transition temperature as high as 24 K appears at a Ce content of $y=0.15$. On the other hand, the existence of an antiferromagnetic order in the rare-earth sublattice was revealed for R_2CuO_4 (R=Nd, Sm, or Gd); moreover, the coexistence of superconductivity and antiferromagnetism of rare-earth ions has been suggested.[8,10,12–16] $R_{2-y}Ce_yCuO_{4-\delta}$ systems seem interesting to study the correlation between superconductivity in the Cu sublattice and antiferromagnetism in the rare-earth sublattice.

In the T'-type oxides of $R_{2-y}Ce_yCuO_{4-\delta}$ (R=Pr, Nd, Sm, Eu, or Gd), superconductivity is not observed when R is Gd. Since the Gd ion has the maximum magnetic moment ($\approx 8\mu_B$) among the rare-earth ions in T'-type oxides, the magnetism of the Gd ion seems to make a considerable contribution to the suppression of superconductivity through a magnetic interaction between rare-earth and copper ions. In order to clarify the reason for the absence of superconductivity in the $Gd_{2-y}Ce_yCuO_{4-\delta}$ system, the superconductivity and magnetism of the $Sm_{1.85-x}Gd_xCe_{0.15}CuO_{4-\delta}$ system were studied, and a possible contribution of the magnetism of Gd ions to the suppression of superconductivity was suggested; moreover, the existence of peculiar successive magnetic transitions, which are observed for specimens with high Gd content and sensitive to the applied magnetic field, was reported.[17,18] The absence of superconductivity was also studied in the $Gd_{2-y}Ce_yCuO_{4-\delta}$ system through magnetic measurement, and the role of an antiferromagnetic order in the Cu sublattice was suggested;[19] however, the reason for the absence as well as the intrinsic magnetic properties of the system seems as yet unclear. Since the magnetic properties of these materials are very sensitive to the intensity of the applied magnetic field, intrinsic magnetic properties must be studied using a very low magnetic field. Although the $Gd_{2-y}Ce_yCuO_{4-\delta}$ system may be a key material for the study, it seems important to study the $Sm_{1.85-x}Gd_xCe_{0.15}CuO_{4-\delta}$ system using single crystals under a wide range of applied magnetic fields for clarifying the interplay between superconductivity and magnetism in T'-type oxides. In the present study, the superconducting and magnetic properties of $Sm_{1.85-x}Gd_xCe_{0.15}CuO_{4-\delta}$ crystals were investigated and compared with those of $Gd_{2-y}Ce_yCuO_{4-\delta}$ crystals.

II. EXPERIMENT

Single crystals of $Sm_{1.85-x}Gd_xCe_{0.15}CuO_{4-\delta}$ and $Gd_{2-y}Ce_yCuO_{4-\delta}$ were prepared by the self-flux method us-

ing excess CuO as a flux. High-purity (99.9%) oxide powders of R_2O_3 (R=Sm, Gd), CeO_2, and CuO were used as raw materials. The content of the CuO flux was changed in the range of 70–78 mol %. An appropriate mixture of R_2O_3, CeO_2, and CuO was charged in a platinum crucible and heated to 1200–1300 °C in an electric furnace. After being held at that temperature for 5 h, it was cooled to 1000–1120 °C at the rate of 1 °C/h, and the furnace was turned off to cool the crucible to room temperature. Crystals were removed mechanically from the flux. To induce superconductivity, specimens of $Sm_{1.85-x}Gd_xCe_{0.15}CuO_{4-\delta}$ were annealed at 950 °C in flowing argon gas. Oxygen deficiency was characterized by iodometry and thermogravimetric analysis. Oxygen deficiency δ in the specimens of $Sm_{1.85-x}Gd_xCe_{0.15}CuO_{4-\delta}$ was kept in the range of 0.03–0.04 by controlling the annealing time from 4 to 24 h.

The chemical composition of the crystals was determined by electron-probe microanalysis (EPMA) using wavelength dispersive spectrometers. The crystal structure was characterized by x-ray powder diffraction and subsequent refinement of the diffraction data using the Rietveld method. The crystallographic directions were determined by the x-ray Laue backreflection method. The Ce concentration in the crystals was also confirmed using the relation between the lattice constants and Ce concentration obtained using polycrystalline specimens. Magnetization measurements were performed at temperatures from 2 to 300 K using a superconducting quantum interference device (SQUID) magnetometer in applied magnetic fields from 5 Oe to 50 kOe. Electrical resistivity was measured by a dc four-probe method at temperatures from 10 to 300 K. Electrical contacts were established by attaching gold wires (50 μm) onto the *ab* plane using silver paint with subsequent annealing in an argon atmosphere at 350 °C for 4 h.

III. RESULTS AND DISCUSSION

A. Properties of $Sm_{1.85-x}Gd_xCe_{0.15}CuO_{4-\delta}$

Through the refinement of the x-ray diffraction data, it was confirmed that all the crystals of $Sm_{1.85-x}Gd_xCe_{0.15}CuO_{4-\delta}$ (δ=0.03–0.04) have a tetragonal T'-phase structure of space group $I4/mmm$. The refined lattice constants [Fig. 1(a)] and interatomic distances [Fig. 1(b)] of $Sm_{1.85-x}Gd_xCe_{0.15}CuO_{4-\delta}$ are shown in Fig. 1 as a function of the Gd content x. For specimens with Gd contents of $0 \leqslant x \leqslant 1.0$, the constants a and c decrease linearly as the Gd content increases. However, they change their behavior above $x=1$. The nearest interatomic distances of Cu-R and Cu-Cu show the same Gd-content dependence as those of the lattice constants. This suggests that the crystal lattice of $Sm_{1.85}Ce_{0.15}CuO_{4-\delta}$ shrinks uniformly by the Gd substitution. The decrease in the lattice parameters appears to be due to the difference in the size of rare-earth ions. Since the ionic radius (0.111 nm) of Gd^{3+} is smaller than that (0.113 nm) of Sm^{3+}, the lattice parameters would decrease as the Gd content increases following Vegard's law. However, the behavior above $x=1$ deviates from the law, suggesting that a change occurs in the crystal lattice.

Figure 2(a) shows the temperature dependence of magnetization measured for specimens of $Sm_{1.85-x}Gd_xCe_{0.15}CuO_{4-\delta}$ under a magnetic field of 5 Oe applied to the *ab* plane. As shown in the figure, the superconducting transition temperature decreases as the Gd content increases, while the paramagnetic contribution increases with increasing the content of Gd. This seems to be due to the paramagnetism of Gd ions. Figure 2(b) shows the temperature dependence of magnetization measured for specimens of $Sm_{1.35}Gd_{0.5}Ce_{0.15}CuO_{4-\delta}$ under a magnetic field of 10 kOe applied parallel to the *c* axis and the *ab* plane of

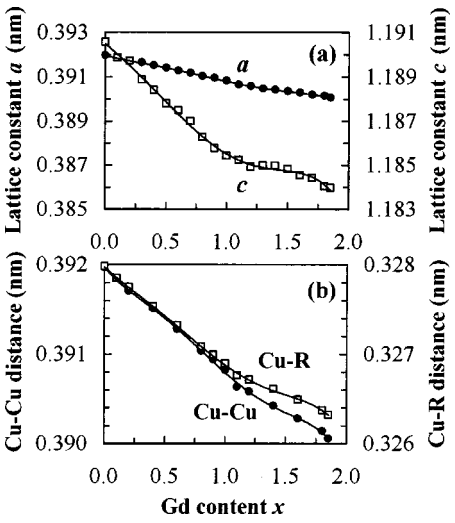

FIG. 1. Gd-content dependence of (a) refined lattice constants and (b) interatomic distances of $Sm_{1.85-x}Gd_xCe_{0.15}CuO_{4-\delta}$.

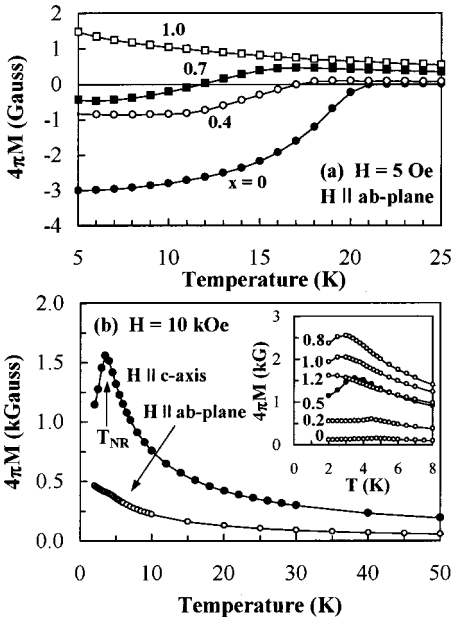

FIG. 2. (a) Temperature dependence of magnetization measured for $Sm_{1.85-x}Gd_xCe_{0.15}CuO_{4-\delta}$ ($x \leqslant 1$) crystals under a magnetic field of 5 Oe applied to the *ab* plane. (b) Temperature dependence of magnetization measured for $Sm_{1.35}Gd_{0.5}Ce_{0.15}CuO_{4-\delta}$ crystal under a magnetic field of 10 kOe applied to the *c* axis and *ab* plane. The inset of the figure shows the data for specimens with $0 \leqslant x \leqslant 1.2$ at temperatures below 8 K.

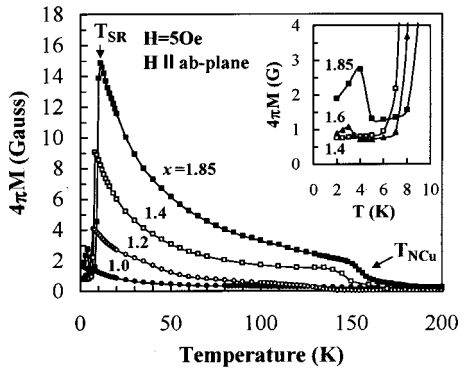

FIG. 3. Temperature dependence of magnetization measured for $Sm_{1.85-x}Gd_xCe_{0.15}CuO_{4-\delta}$ ($x>1.0$) crystals under a magnetic field of 5 Oe applied to the *ab* plane. The inset of the figure shows the data for specimens with $x=1.4$, 1.6, and 1.85 at temperatures below 10 K.

tetragonal crystals. A peak, which resembles the antiferromagnetic transition, is observed when the magnetic field is applied parallel to the *c* axis. In neutron diffraction studies for Sm_2CuO_4, it was reported that a long-range antiferromagnetic order of Sm spins was observed in the direction parallel to the *c* axis at about 6 K.[10,20] In general, an antiferromagnetic peak appears in the geometry in which antiferromagnetically coupled moments are parallel to the applied magnetic field. Therefore, if the observed magnetization is due to rare-earth moments, the antiferromagnetic order of rare-earth ions must be parallel to the *c* axis for crystals with high Sm concentration. This is consistent with the result of neutron diffraction studies. The inset of Fig. 2(b) shows the temperature dependence of magnetization measured for specimens with various Gd contents at 10 kOe. The peak (hereafter the peak temperature is referred to as T_{NR}), which is observed for specimens with a Gd content of $0\leqslant x\leqslant 1$, shifts to lower temperatures as the Gd content increases and cannot be observed for specimens with $x>1$ at temperatures down to 2 K. This decrease in T_{NR} seems to be due to the preferential direction of rare-earth spins. It is accepted that Sm spins are parallel to the *c* axis in Sm_2CuO_4, while Gd spins are parallel to the *ab* plane in Gd_2CuO_4.[10,15] Since Gd spins are perpendicular to Sm spins in the $Sm_{1.85-x}Gd_xCe_{0.15}CuO_{4-\delta}$ system, the magnetic interaction between Sm and Gd spins must be weaker than that among Sm spins. Therefore, Gd substitution will dilute the magnetic interaction among Sm spins, and T_{NR} due to the Sm spins will then decrease with increasing the content of Gd.

Figure 3 shows the temperature dependence of magnetization measured for specimens of $Sm_{1.85-x}Gd_xCe_{0.15}CuO_{4-\delta}$ ($x\geqslant 1$) under a magnetic field of 5 Oe applied parallel to the *ab* plane. New magnetic transitions appear in the temperature ranges of 2–10 K and 130–170 K. The magnetization observed for specimens with a Gd content of $x>1$ at temperatures between 10 and 170 K is considerably larger than that expected for Cu ions and behaves like a ferromagnet. The transition observed at higher temperatures (130–170 K) is considered to be an antiferromagnetic (or weak-ferromagnetic) transition in the Cu sublattice, which has been observed in the neutron diffraction studies for R_2CuO_4 ($R=$ Nd, Pr, or Sm).[2–11] This transition (hereafter referred to as T_{NCu}) shifts to higher temperatures with increasing the content of Gd. This behavior is consistent with that observed for $Sm_{2-x}Gd_xCuO_{4-\delta}$ (Ref. 21) and seems to be due to the change in the crystal structure, which has been shown in Fig. 1. Since the lattice constants and Cu-Cu distance decrease with increasing content of Gd, T_{NCu} would increase by enhancement of the magnetic interaction between Cu spins. The transitions at temperatures between 6 and 20 K (hereafter the peak temperature is referred to as T_{SR}) shift to higher temperatures as the Gd content increases. The shape of the thermomagnetic curve depends strongly on the Gd content and the intensity of the applied magnetic field. The behavior of magnetization, which is observed for specimens with a Gd content of $x>1$ at temperatures between T_{SR} and T_{NCu}, is considered to be due to the weak ferromagnetism in the Cu sublattice. In general, weak ferromagnetism does not occur in magnetic oxides with high crystal symmetry. However, the lattice constants of $Sm_{2-x}Gd_xCe_xCuO_{4-\delta}$ change their behavior at about $x=1$. This change in the lattice constants seems to have a close relation to the behavior of magnetization. If the crystal lattice starts to distort at about $x=1$, weak ferromagnetism may occur through the deterioration of the crystal symmetry. In addition, $x=1$ is the critical composition at which Gd ions take over the main role from Sm ions. As mentioned above, in the R_2CuO_4-type oxides, Sm and Gd spins have an antiferromagnetic order in the directions parallel to the *c* axis and *ab* plane, respectively, below Néel temperature. Therefore, although rare-earth spins are paramagnetic at temperatures above T_{NR}, it is likely that Gd spins still remain in the *ab* plane and affect the weak ferromagnetism through a magnetic interaction between Cu and Gd spins. The decrease in the Cu-*R* distance, which has been shown in Fig. 1, may enhance the magnetic interaction between the Cu and Gd spins and the weak ferromagnetism. When the Gd content exceeds $x=1.5$, another transition appears at temperatures of 2–5 K. This peak (hereafter the peak temperature is referred to as T_{NGd}) appears to be an antiferromagnetic transition in the Gd sublattice. In the magnetic susceptibility, neutron diffraction, electron paramagnetic resonance (EPR), and specific heat measurements for Gd_2CuO_4, a peak due to antiferromagnetic transition in the Gd sublattice has been reported at temperatures between 6 and 9 K when the magnetic field was applied parallel to the CuO_2 plane (or *ab* plane).[12,15,16,22–24] Therefore, it is considered that, in the $Sm_{1.85-x}Gd_xCe_{0.15}CuO_{4-\delta}$ system, the antiferromagnetic order of Sm spins, which is parallel to the *c* axis, is suppressed by the Gd substitution and a new antiferromagnetic order due to Gd spins appears in the *ab* plane as the Gd content increases over $x=1$. Details of these transitions at T_{SR} and T_{NGd} will be given in the next section.

Figure 4(a) shows the temperature dependence of reciprocal susceptibility $1/\chi$ measured for specimens of $Sm_{1.25}Gd_{0.6}Ce_{0.15}CuO_{4-\delta}$ in the *ab* plane. $1/\chi$ of the *ab* plane shows a linear temperature dependence and can be fitted by the Curie-Weiss law given by $\chi^{-1}=(T+\Theta)/C$, where Θ and *C* are the asymptotic Curie temperature and Curie con-

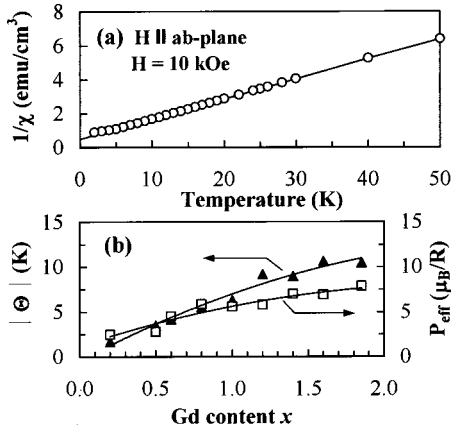

FIG. 4. (a) Temperature dependence of reciprocal susceptibility χ^{-1} for $Sm_{1.25}Gd_{0.6}Ce_{0.15}CuO_{4-\delta}$ crystal and (b) Gd-content dependence of asymptotic Curie temperature Θ and effective paramagnetic moment $P_{\rm eff}$.

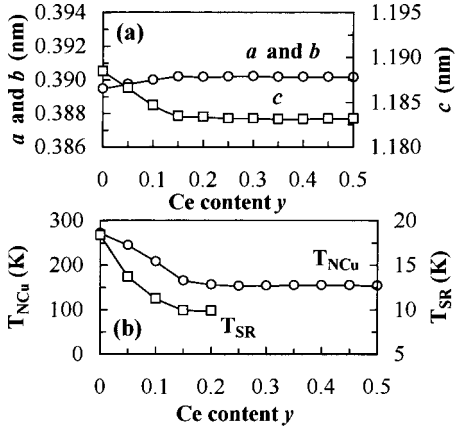

FIG. 5. Ce-content dependence of (a) tetragonal lattice parameters a and c and (b) transition temperatures $T_{\rm NCu}$ and $T_{\rm SR}$ for specimens of $Gd_{2-y}Ce_yCuO_{4-\delta}$.

stant, respectively. $\Theta=-4.17$ K and $C=0.085$ were obtained by fitting the above equation to the data. The fitting was also done for specimens with various Gd contents. Figure 4(b) shows the asymptotic Curie temperature Θ and the effective paramagnetic moment $P_{\rm eff}$, which is deduced from the Curie constant C, as a function of Gd content x. Here Θ is always negative, and its absolute value increases as the Gd content increases. This result suggests that the antiferromagnetic interaction among rare-earth ions is enhanced by the Gd substitution. Since the magnetic moment of the Gd ion is lager than that of the Sm ion, the exchange interaction between rare-earth ions must be enhanced. On the other hand, $P_{\rm eff}$ is considerably large and increases as the Gd content increases. It is well known that the magnetic moment of the Cu ion is very small in R_2CuO_4-type oxides. Therefore, the $P_{\rm eff}$ observed for $Sm_{2-x}Gd_xCe_xCuO_{4-\delta}$ can be attributed to the magnetic moment of rare-earth ions. The values of $P_{\rm eff}$ agree well with those calculated by assuming the theoretical magnetic moments of $0.84\mu_B$ and $7.94\mu_B$ for Sm^{3+} and Gd^{3+}, respectively.

B. Properties of $Gd_{2-y}Ce_yCuO_{4-\delta}$

Figure 5(a) shows the Ce-content dependence of tetragonal lattice parameters a and c for specimens of $Gd_{2-y}Ce_yCuO_{4-\delta}$. Data for single crystals with a Ce content of $y\leqslant 0.15$ are shown, together with those for polycrystals with a nominal Ce content of $y>0.15$. The lattice parameters a and c are almost constant for specimens with a Ce content of $y>0.15$. This is consistent with the result of Ref. 19. Figure 5(b) shows the Ce content dependence of the antiferromagnetic transition temperature $T_{\rm NCu}$ and the spin-reorientation temperature $T_{\rm SR}$, which were determined from the thermomagnetic curves measured under a magnetic field of 10 Oe. $T_{\rm NCu}$ and $T_{\rm SR}$ decrease to lower temperatures with increasing the content of Ce, however, they approach a fixed value in specimens with a Ce content of $y>0.15$. These behaviors are very similar to that of the lattice constant c and suggest that the solubility limit of Ce is found in the vicinity of $y=0.15$. It is well known that the Ce ion exists as a nonmagnetic Ce^{4+} ion in the superconducting $R_{2-y}Ce_yCuO_{4-\delta}$ (R=Pr, Nd, and Sm). Therefore, it seems natural to consider that the Ce ion exists as a Ce^{4+} ion in $Gd_{2-y}Ce_yCuO_{4-\delta}$. Since the oxygen deficiency has been kept in the range of 0.03–0.04, the valence state of Cu ions must be changed by the substitution of Ce^{4+} ions, and then the nonmagnetic Cu^{+} ion will be introduced. The decrease observed for $T_{\rm NCu}(y)$ and $T_{\rm SR}(y)$ would be due to the valence change of Cu ions.

Figure 6 shows the temperature dependence of the magnetization measured for a crystal of $Gd_{1.85}Ce_{0.15}CuO_{4-\delta}$, which is the end member of the $Sm_{1.85-x}Gd_xCe_{0.15}CuO_{4-\delta}$ system, under a magnetic field of 10 Oe applied parallel to the c axis and ab plane. The magnetization observed in the c axis is very small and shows a monotonous decrease with increasing the temperature. However, when a magnetic field is applied parallel to the ab plane, distinct magnetic transitions are observed at 4, 10, and 160 K, and as shown in the inset of the figure, the transitions at 4 and 10 K show a thermal hysteresis during the heating and cooling processes. These transitions are hereafter referred to as transitions A, B,

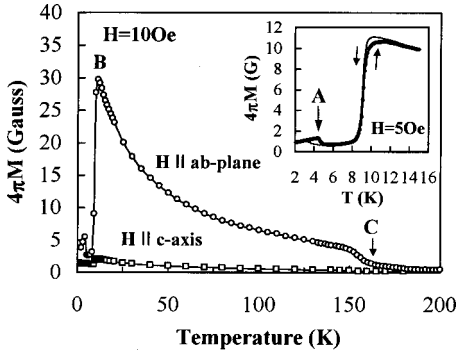

FIG. 6. Temperature dependence of the magnetization measured for $Gd_{1.85}Ce_{0.15}CuO_{4-\delta}$ crystal under a magnetic field of 10 Oe applied parallel to the c axis and ab plane. The inset of the figure shows the data measured in the vicinity of transitions A and B under a magnetic field of 5 Oe applied to the ab plane.

and *C*, and the phases between these transitions are referred to as phases I, II, III, and IV. Transition *A*, which has been observed for specimens of $Sm_{1.85-x}Gd_xCe_{0.15}CuO_{4-\delta}$ ($x \geqslant 1.6$) and characterized by T_{NGd}, is an antiferromagnetic transition occurring in the Gd sublattice. On the other hand, transitions *B* and *C*, respectively, correspond to the spin-reorientation and the antiferromagnetic transitions, which have been characterized by T_{SR} and T_{NCu} in the results of the magnetization measurement for $Sm_{1.85-x}Gd_xCe_{0.15}CuO_{4-\delta}$.

Following the theoretical studies of the magnetism of orthochromite and orthoferrite systems,[25] the Hamiltonian of the $(Gd,Ce)_2CuO_4$ system is given by $\mathcal{H}=\mathcal{H}_{Cu}+\mathcal{H}_{Cu\text{-}Gd}+\mathcal{H}_{Gd}$, where $\mathcal{H}_{Cu}$, $\mathcal{H}_{Gd}$, and $\mathcal{H}_{Cu\text{-}Gd}$ are the Hamiltonians of Cu and Gd ions and the interaction between Cu and Gd ions, respectively. The Hamiltonian $\mathcal{H}_{Cu}$ is given by $\mathcal{H}_{Cu}=\mathcal{H}_{iso}+\mathcal{H}_{anti}+\mathcal{H}_{symm}+\mathcal{H}_{an}$, where $\mathcal{H}_{iso}$, $\mathcal{H}_{anti}$, and $\mathcal{H}_{symm}$ are the Hamiltonians of the isotropic exchange interaction $\Sigma_{i\neq j}J_{ij}\mathbf{S}_i^{Cu}\cdot\mathbf{S}_j^{Cu}$, the antisymmetric exchange interaction $\Sigma_{i\neq j}\mathbf{D}_{ij}\cdot\mathbf{S}_i^{Cu}\times\mathbf{S}_j^{Cu}$, and the anisotropic-symmetric exchange interactions $\Sigma_{i\neq j}\mathbf{S}_i^{Cu}\cdot\mathbf{a}_{ij}\cdot\mathbf{S}_j^{Cu}$ between Cu ions, respectively, and $\mathcal{H}_{an}$ is the one-ion anisotropy energy $DS_z^2+E(S_x^2-S_y^2)$ of Cu ions. Therefore, the Hamiltonian $\mathcal{H}_{Cu}$ is further given by

$$\mathcal{H}_{Cu}=\sum_{i\neq j}\left(J_{ij}\mathbf{S}_i^{Cu}\cdot\mathbf{S}_j^{Cu}+\mathbf{D}_{ij}\cdot\mathbf{S}_i^{Cu}\times\mathbf{S}_j^{Cu}+\mathbf{S}_i^{Cu}\cdot\mathbf{a}_{ij}\cdot\mathbf{S}_j^{Cu}\right)+DS_z^2+E(S_x^2-S_y^2).$$

At temperatures between T_{NCu} and T_{SR}, the easy axis of magnetization of Cu spins is determined by the one-ion magnetic anisotropy of Cu ions, the Cu spins are aligned antiferromagnetically along the [110] direction by the isotropic exchange interaction, and a weak-ferromagnetic moment is induced by the antisymmetric exchange interaction (or Dzyaloshinsky-Moriya interaction[26]), which tilts Cu spins toward the [001] direction (overt canting) and spreads them out along the *ab* plane (hidden canting). However, x-ray diffraction studies have revealed that $Gd_{1.85}Ce_{0.15}CuO_4$ has a tetragonal structure of space group $I4/mmm$, and weak ferromagnetism due to the antisymmetric exchange interaction cannot be expected for crystals with a high symmetry such as $I4/mmm$. Although the existence and the effect of local distortion have been proposed to explain the occurrence of weak ferromagnetism in Gd_2CuO_4 and related oxides,[12,16,21,27–29] the details of the distortion and magnetism in $Gd_{1.85}Ce_{0.15}CuO_4$ still remained unclear. Figure 7 shows the electron diffraction pattern for the (001) plane (or the *ab* plane) of a $Gd_{1.85}Ce_{0.15}CuO_4$ crystal. Small extra spots are observed among clear main spots. This is strong evidence of a lattice distortion existing in $Gd_{1.85}Ce_{0.15}CuO_4$ crystals. The diffraction pattern can be explained by assuming the orthorhombic space group *Bmab*. A small distortion of the oxygen site in the *ab* plane is considered to deteriorate the crystal symmetry. The orthorhombic lattice parameter a^* (or b^*) of space group *Bmab* has a relation of $a^*=\sqrt{2}a$ with tetragonal lattice parameter *a* of space group $I4/mmm$. Possible lattice distortion models that explain the electron diffraction pattern with orthorhombic symmetry are shown in Fig. 7. Each model has an alternative lattice distortion in the CuO_2 plane; however, the position of Cu ions is independent of the lattice distortion. Among these models, (b) most likely exists in $Gd_{1.85}Ce_{0.15}CuO_4$ crystals. When the middle point (point *M*) of a line between Cu ions is the center of inversion symmetry, **D** is equal to zero. This is the case for tetragonal crystals of space group $I4/mmm$. Since the point *M* is a center of inversion symmetry, weak ferromagnetism due to the antisymmetric exchange interaction cannot be expected. However, when a lattice distortion occurs in a tetragonal crystal and the crystal has an orthorhombic structure of space group *Bmab*, weak ferromagnetism may occur in $Gd_{1.85}Ce_{0.15}CuO_4$ since point *M* is no longer a center of inversion symmetry. Therefore, the magnetism observed at temperatures between T_{SR} and T_{NCu} (phase III) is considered to be weak ferromagnetism.

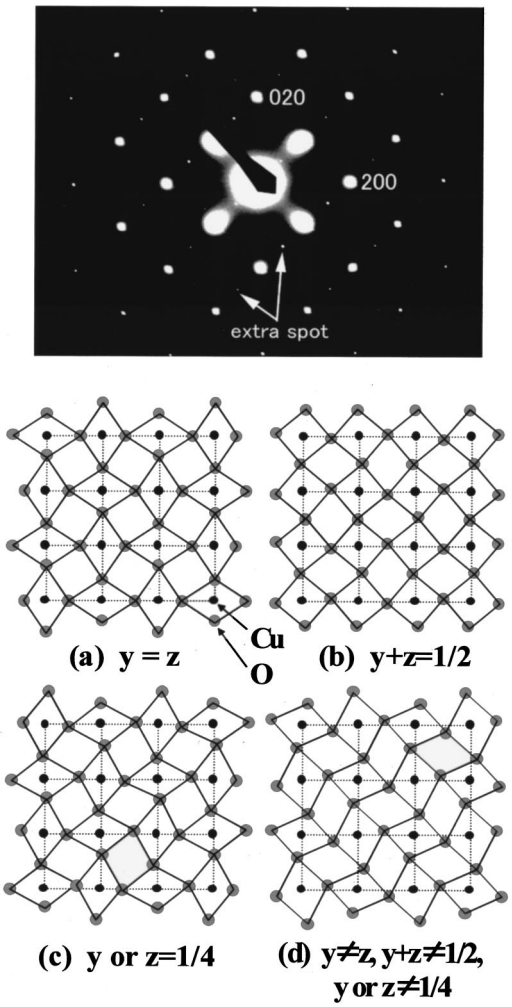

FIG. 7. Electron diffraction pattern for the (001) plane (or *ab* plane) of $Gd_{1.85}Ce_{0.15}CuO_{4-\delta}$ crystal. The incident electron beam is parallel to the [001] direction. (a), (b), (c), and (d) show possible models that explain the orthorhombic lattice distortion observed in the diffraction data.

Figure 8(a) shows the temperature dependence of magnetization measured for the same crystal under various magnetic fields applied parallel to the *c* axis. In this case, al-

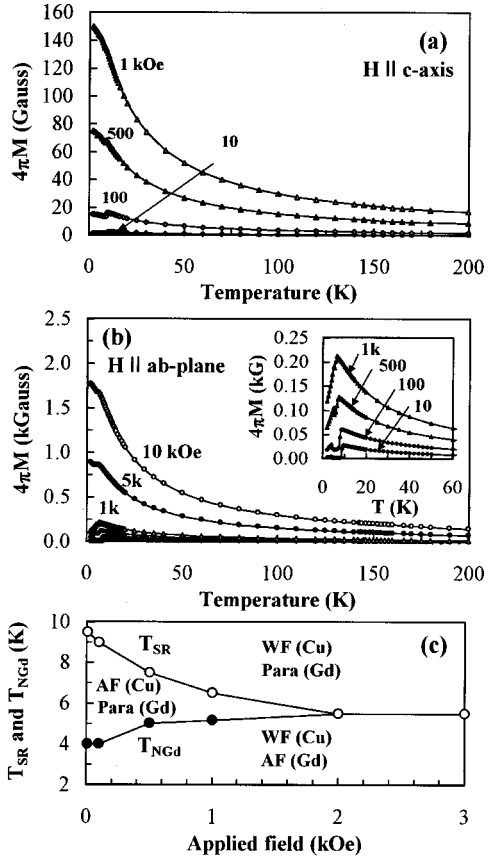

FIG. 8. Temperature dependence of magnetization measured for $Gd_{1.85}Ce_{0.15}CuO_{4-\delta}$ crystal under various magnetic fields applied parallel to (a) the *c* axis and (b) the *ab* plane. The inset of (b) shows the data measured under a magnetic field between 10 and 1 kOe. (c) shows the field dependence of transition temperatures T_{NGd} and T_{SR}.

though a small anomaly is observed at about 10 K, magnetization shows a monotonous decrease as the temperature is increased. Figure 8(b) shows the temperature dependence of magnetization measured under various magnetic fields applied parallel to the *ab* plane. Transitions observed at low temperatures are affected considerably by the applied magnetic field. When the field intensity is increased, transition *B* (at T_{SR}), at which the antiferromagnetic spin configuration in the Cu sublattice is reoriented to form a weak-ferromagnetic order, shifts to lower temperatures and coincides with transition *A* (at T_{NGd}) at an applied field of ~2 kOe to form a single peak near 6 K. When a magnetic field over 3 kOe is applied, the peak becomes indistinct; furthermore, magnetization increases monotonously with descending the temperature, and a shoulder is observed near 6 K. A magnetic phase diagram for a specimen of $Gd_{1.85}Ce_{0.15}CuO_4$ at low temperature is shown in Fig. 8(c). In the phase between T_{SR} and T_{NGd}, Cu and Gd spins are considered to exist in an antiferromagnetic and a paramagnetic state, respectively. This phase disappears at a magnetic field above 2 kOe. This seems to be due to a field-induced spin reorientation of Cu spins. When the field intensity increases, the antiferromagnetically ordered Cu spins, which are very sensitive to the applied magnetic field, reorient to form a weak-ferromagnetic spin configuration, which is the same magnetic structure as that in phase III. The decrease in $T_{SR}(H)$ is attributed to the expansion of the weak-ferromagnetic phase (phase III) to lower temperatures with the assistance of the applied magnetic field. On the other hand, paramagnetic Gd spins in phase II are aligned by an internal magnetic field, which is induced by the formation of a weak-ferromagnetic spin configuration in the Cu sublattice through field-induced spin reorientation, and make a great contribution to the magnetization. This is why magnetization in phase II increases as the applied field increases.

The magnetization observed in the *ab* plane at temperatures between T_{SR} and T_{NCu} is considerably larger than that expected for Cu ions. The magnetization is attributed to the moment of Gd ions. Figures 9(a) and 9(b) show the temperature dependence of reciprocal magnetic susceptibility χ^{-1} measured in various magnetic fields applied parallel to the *ab* plane and *c* axis, respectively. The $\chi^{-1}(T)$ shows linear temperature dependence at temperatures between 10 and 150 K, and the linear part of the curve can be fitted by the Curie-Weiss law. Figure 9(c) shows the field dependence of effective magnetic moment P_{eff}, which is calculated from the Curie constant obtained by the fitting. P_{eff} decreases considerably at a low magnetic field and approaches the constant value ($\approx 7.9\mu_B$) at higher magnetic fields. This value is consistent with the theoretical value ($7.94\mu_B$) for the free Gd ion. From the results shown in Figs. 8 and 9, it is supposed that, in phase III, the paramagnetic moments of Gd ions are aligned by an internal magnetic field induced by a spontane-

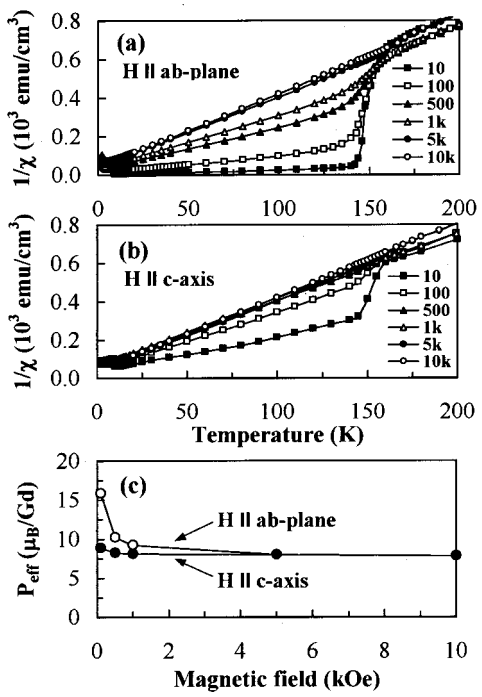

FIG. 9. Temperature dependence of reciprocal magnetic susceptibility χ^{-1} measured for $Gd_{1.85}Ce_{0.15}CuO_{4-\delta}$ crystal in the various magnetic fields applied parallel to (a) the *ab* plane and (b) the *c* axis, and (c) field dependence of effective magnetic moment P_{eff}, which is calculated from the Curie constant obtained by fitting the Curie-Weiss law to the linear portion of $\chi^{-1}(T)$.

ous weak-ferromagnetic (WF) moment that is brought on by a canting of antiferromagnetically coupled moments of Cu ions. Taking the theoretical considerations by Yamaguchi for RMO_3 (R=rare earth, M=Fe or Cr) into account, the Hamiltonian of the interaction between Cu and Gd ions in the $(Gd,Ce)_2CuO_4$ system would be represented by

$$\mathcal{H}_{\text{Cu-Gd}}=\sum_{i\neq j}\left(\tilde{J}_{ij}\mathbf{S}_i^{\text{Cu}}\cdot\mathbf{S}_j^{\text{Gd}}+\tilde{\mathbf{D}}_{ij}\cdot\mathbf{S}_i^{\text{Cu}}\times\mathbf{S}_j^{\text{Gd}}+\mathbf{S}_i^{\text{Cu}}\cdot\tilde{\mathbf{a}}_{ij}\cdot\mathbf{S}_j^{\text{Gd}}\right)$$

using the isotropic, the antisymmetric, and the anisotropic-symmetric exchange interactions between Cu and Gd ions.[25] Gd spins are aligned antiparallel to the weak-ferromagnetic moment through the interaction $\Sigma_{i\neq j}\tilde{J}_{ij}\mathbf{S}_i^{\text{Cu}}\cdot\mathbf{S}_j^{\text{Gd}}$. This interaction can be represented in terms of an interaction between an effective magnetic field H_i and the spin moment of the Gd ion, which is given by $E=-\alpha M_{\text{Cu}}M_{\text{Gd}}=-H_iM_{\text{Gd}}$. This effective field corresponds to the internal field mentioned above. When the spin moment of the rare-earth ion increases as the temperature is lowered, the isotropic exchange interaction $\Sigma_{i\neq j}\tilde{J}_{ij}\mathbf{S}_i^{\text{Cu}}\cdot\mathbf{S}_j^{R}$ is enhanced, and then the effective magnetic field H_i is increased. The magnitude of the WF moment as well as the canting angle depends on the intensity of the applied magnetic field. When the WF moment is enhanced by the applied magnetic field and Gd moments are aligned completely in the direction of internal magnetic field, the effective moment P_{eff} becomes constant. This must be why large magnetization is observed in the *ab* plane at temperatures between T_{SR} and T_{NCu}, the magnetization depending strongly on the Gd content and the intensity of the applied magnetic field.

In order to describe the magnetism of $Gd_{1.85}Ce_{0.15}CuO_4$ in detail, the field dependence of magnetization was measured at some characteristic temperatures in phases I, II, III, and IV. Figure 10(a) shows the field dependence of magnetization measured for $Gd_{1.85}Ce_{0.15}CuO_4$ at 200 K in phase IV by applying a magnetic field parallel to the *ab* plane. The $M(H)$ curve shows linear and reversible field dependence, suggesting the existence of paramagnetism at temperatures above T_{NCu} (or transition C). This behavior is independent of the field direction. Figure 10(b) shows magnetization curves $M(H)$ measured at various temperatures in phase III under a magnetic field applied parallel to the [100] direction in the *ab* plane (hereafter direction is represented by the tetragonal symmetry of space group $I4/mmm$). The magnetization tends to be saturated at a very low magnetic field ($H<200$ Oe) and shows linear field dependence at higher magnetic fields. In addition, a magnetic hysteresis was observed in the $M(H)$ curves. The $M(H)$ curves in the [110] direction show the same behavior as those in the [100] direction. This behavior of the $M(H)$ curves resembles that of weak ferromagnetism. When weak ferromagnetism is established in $Gd_{1.85}Ce_{0.15}CuO_4$, the $M(H)$ curve is represented by

$$M(H)=M_{\text{Cu}}+C_{\text{Gd}}\frac{H_i+H}{T+\Theta}, \tag{1}$$

where M_{Cu}, C_{Gd}, H_i, and Θ are the spontaneous weak-ferromagnetic moment induced by a canting of Cu spins, the Curie constant of Gd, the internal field acting on Gd sites, and the asymptotic Curie temperature, respectively.[30] C_{Cu} has been ignored because C_{Gd} appears to be much larger than C_{Cu}. H_i and M_{Cu} can be determined from the $M(H)$ curves measured at different temperatures between 20 and 130 K using Eq. (1). The extrapolation of the linear portion of $M(H)$ curves, which are measured at neighboring temperatures, intersects at a point, indicating $H=H_i$ and $M=M_{\text{Cu}}$. Here $H_i=-426$ Oe and $M_{\text{Cu}}=(4.2\times10^{-3})\mu_B$ were obtained from the $M(H)$ curves measured at 20 and 50 K. The negative sign of H_i indicates that the internal field acting on the Gd site is antiparallel to the direction of the applied magnetic field. These values are consistent with those reported for Gd_2CuO_4.[19,22,31,32] Since paramagnetic Gd moments are aligned by H_i, significantly large magnetization can be observed even in a low applied magnetic field of 10 Oe. Here H_i at each temperature can be estimated by neglecting the M_{Cu} in Eq. (1). In this case, a point where the linear extrapolation of the $M(H)$ curve intersects the abscissa gives H_i. The absolute value of H_i is shown in Fig. 11(a) as a function of the temperature. H_i shows a remarkable decrease in the vicinity of T_{NCu}. Moreover, it is seen that H_i along the c axis is about one-tenth of that in the *ab* plane. These facts apparently indicate that the WF moment, which is due to a canting of Cu moments, exists in the *ab* plane at temperatures between T_{SR} and T_{NCu}. Figure 11(b) shows the Gd-content dependence of H_i obtained for specimens of $Sm_{1.85-x}Gd_xCe_{0.15}CuO_{4-\delta}$ at 50 K by applying a magnetic field parallel to the [100] direction. H_i appears for specimens with a Gd content of $x>1$, while the superconductivity disappears for these specimens. Although the occurrence of weak ferromagnetism is attributed to the lattice distortion

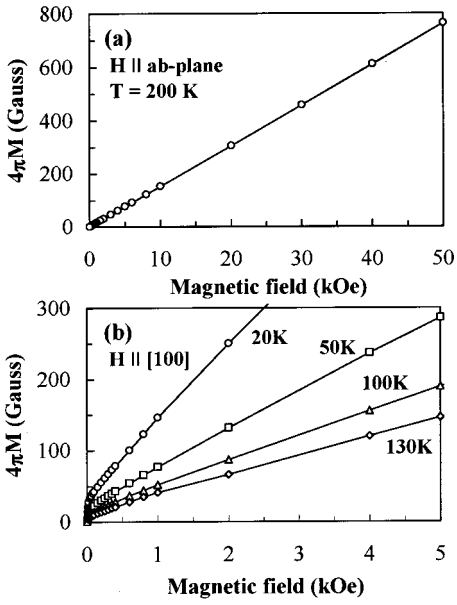

FIG. 10. (a) Field dependence of magnetization measured for $Gd_{1.85}Ce_{0.15}CuO_{4-\delta}$ crystal at 200 K by applying a magnetic field parallel to the *ab* plane and (b) field dependence of magnetization measured at various temperatures in phase III under a magnetic field applied parallel to the [100] direction in the *ab* plane.

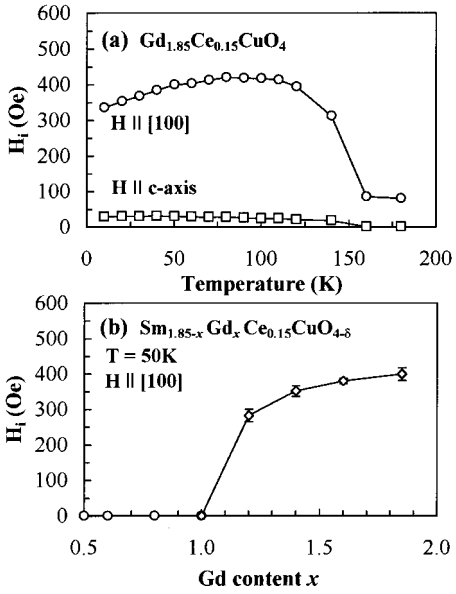

FIG. 11. (a) Temperature dependence of internal field H_i estimated from the field dependence of magnetization measured for $Gd_{1.85}Ce_{0.15}CuO_{4-\delta}$ crystal at various temperatures. (b) Gd-content dependence of internal field H_i obtained from the magnetization curves measured for $Sm_{1.85-x}Gd_xCe_{0.15}CuO_{4-\delta}$ crystals in the [100] direction at 50 K.

that is caused by the Gd substitution, the role of the magnetic interaction between Cu and Gd cannot be disregarded. Unlike Sm spins, which are parallel to the *c* axis and perpendicular to the Cu spins, Gd spins seem to exist in the *ab* plane, at which weak-ferromagnetic Cu spins exist; thus, the magnetic interaction between Cu and Gd spins is expected to be much stronger than that between Cu and Sm spins. Therefore, the magnetic interaction between Cu and Gd may contribute to the occurrence of weak ferromagnetism and the suppression of superconductivity observed for specimens of $Sm_{1.85-x}Gd_xCe_{0.15}CuO_{4-\delta}$ ($x<1$).

Figure 12 shows the angular dependence of magnetization measured for $Gd_{1.85}Ce_{0.15}CuO_4$ at 3, 6, and 20 K, respectively, in phases I, II, and III under a magnetic field of 20 Oe applied parallel to the *ab* plane. Here θ is an angle from the

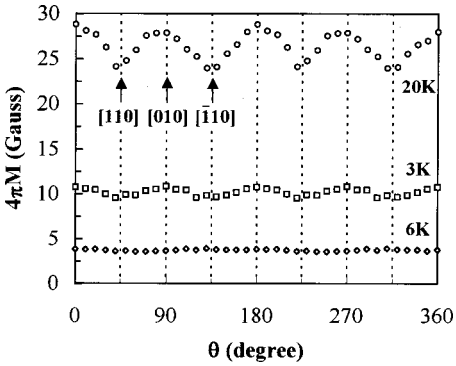

FIG. 12. Angular dependence of magnetization measured for $Gd_{1.85}Ce_{0.15}CuO_4$ crystal at 3, 6, and 20 K, respectively, in phases I, II, and III under a magnetic field of 20 Oe applied parallel to the *ab* plane.

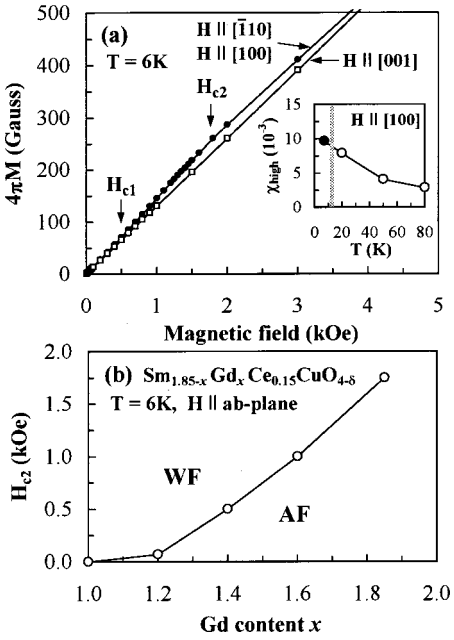

FIG. 13. (a) Field dependence of magnetization measured for $Gd_{1.85}Ce_{0.15}CuO_{4-\delta}$ crystal at 6 K (in phase II) by applying a magnetic field to the [001] (*c*-axis) direction and [100] and [$\bar{1}$10] directions in the *ab* plane. The inset of the figure shows the high-field susceptibility measured in the [100] direction of $Gd_{1.85}Ce_{0.15}CuO_4$ crystal at various temperatures in phase III (open circle) and 6 K (solid circle). (b) Gd-content dependence of the critical field H_{c2} obtained from the magnetization curves measured for $Sm_{1.85-x}Gd_xCe_{0.15}CuO_{4-\delta}$ crystals in the *ab* plane at 6 K.

[100] direction. Magnetization shows anisotropic behavior at 3 and 20 K, and the maximum and minimum are observed at angles that correspond to the ⟨110⟩ and ⟨100⟩ directions, respectively. However, the difference between the maximum and minimum is much smaller at 3 K than at 20 K. On the other hand, there is little angular dependence at 6 K. The $M(\theta)$ curve at 20 K can be explained qualitatively assuming a single magnetic domain. In the domain, antiferromagnetically coupled Cu spins align parallel to one of the ⟨110⟩ directions, and a slight canting of the spins from the ⟨110⟩ direction induces a spontaneous WF moment in the direction perpendicular to the Cu spins. Paramagnetic Gd spins are aligned in the direction of internal magnetic field H_i, which is induced by the WF moment. Since the magnetic moment of Cu ions is negligibly smaller than that of Gd ions, magnetization due to Gd spins, which are aligned by H_i, can be observed in the magnetization measurement. When the applied magnetic field is rotated from the [110] direction and goes across the [010] direction, the spontaneous WF moment lying in the [110] direction switches to the [$\bar{1}$10] direction, which is the nearest direction to the applied field. Since the switching occurs under an applied field that is much smaller than the internal magnetic field H_i, a maximum and minimum of magnetization must be observed when the magnetic field of 20 Oe is applied parallel to the ⟨110⟩ and ⟨100⟩ directions, respectively.

Figure 13(a) shows the field dependence of magnetization measured for $Gd_{1.85}Ce_{0.15}CuO_4$ at 6 K in phase II by apply-

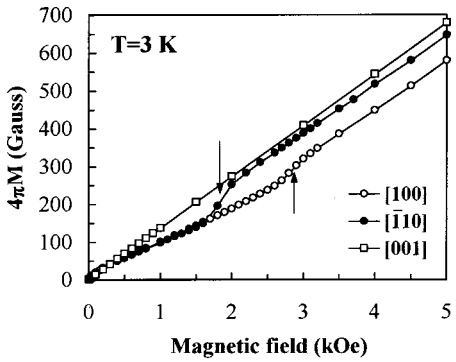

FIG. 14. Field dependence of magnetization measured for $Gd_{1.85}Ce_{0.15}CuO_4$ crystal at 3 K (in phase I) by applying a magnetic field to the [100], [$\bar{1}$10], and [001] directions.

ing a magnetic field to the [001] ($=c$ axis), [100], and [$\bar{1}$10] directions in the *ab* plane. The $M(H)$ curve in the [001] direction shows a linear field dependence, while those in the [100] and [$\bar{1}$10] directions change their slope at $H_{c1}=0.5$ kOe and $H_{c2}=1.8$ kOe. This seems to be a field-induced magnetic phase transition that begins near 0.5 kOe and finishes at about 1.8 kOe. The magnetic susceptibility measured in the [100] (or [$\bar{1}$10]) direction above and below 1.8 kOe is $\chi_{high}=9.66\times10^{-3}$ emu/cm^3 and $\chi_{low}=11.48\times10^{-3}$ emu/cm^3, respectively. The inset of the figure shows the temperature dependence of magnetic susceptibility measured in the [100] direction at temperatures in phase III. It is seen that the χ_{high} at 6 K agrees well with the extrapolation of the $\chi(T)$ curve measured above 10 K. Therefore, it is likely that the antiferromagnetic configuration of Cu spins in phase II, changes into the same canted spin arrangement as that in phase III at magnetic fields between H_{c1} and H_{c2}. On the other hand, Gd spins appear to be paramagnetic in phase II at magnetic fields below H_{c1}. This is clear from the result shown in Fig. 12, in which no angular dependence is observed at 6 K under a field of 20 Oe. However, when the canted spin configuration of Cu ions is established at magnetic fields above H_{c2}, paramagnetic Gd spins align in the direction of H_i, which is induced by the WF moment, and contribute to the magnetization of the specimen. Figure 13(b) shows the Gd-content dependence of the critical field H_{c2} obtained for specimens of $Sm_{1.85-x}Gd_xCe_{0.15}CuO_{4-\delta}$ at 6 K. Here H_{c2} increases monotonously above $x>1$, suggesting that the antiferromagnetic configuration of Cu spins in phase II becomes more stable to the applied field by the Gd substitution. The magnetic interaction between Cu and Gd spins seems to stabilize the antiferromagnetic spin configuration of Cu ions and suppress the field-induced spin-reorientation transition from an antiferromagnetic to a weak-ferromagnetic state.

Figure 14 shows the field dependence of magnetization measured for $Gd_{1.85}Ce_{0.15}CuO_4$ at 3 K in phase I by applying a magnetic field to the [100], [$\bar{1}$10], and [001] directions. The magnetization in the [100] and [$\bar{1}$10] directions rises remarkably as the applied field increases and tends to be saturated at about 200 Oe. However, the magnetization shows a linear field dependence with a further increase in the magnetic field, and jumps are observed at 1.8 and 2.7 kOe, respectively, in the [$\bar{1}$10] and [100] directions. Moreover, the $M(H)$ curve changes its slope before and after the jumps. On the other hand, the $M(H)$ curve in the [001] direction shows linear field dependence up to 50 kOe. The behavior of the $M(H)$ curves is explained qualitatively by a model in which Cu, spins align antiferromagnetically in the axis parallel to the [110] direction, inducing a spontaneous WF moment in the [$\bar{1}$10] direction, while Gd spins align antiferromagnetically in the axis parallel to the [$\bar{1}$10] direction. The weak-ferromagnetic spin configuration in the Cu sublattice is the same as that of phase III. In this case, the field dependence of magnetization is given by

$$M(H)=M_{Cu}+(\chi_{Cu}+\chi_{Gd})H, \tag{2}$$

where M_{Cu}, χ_{Cu}, and χ_{Gd} are the spontaneous WF moment due to Cu spins and the antiferromagnetic susceptibility of Cu and Gd sublattices, respectively. The initial increase in the $M(H)$ curve is attributed to the M_{Cu}, and a single-domain structure is attained in this process. When a magnetic field H with an intensity below 1.8 kOe is applied to the [$\bar{1}$10] direction, a WF moment due to canting Cu spins aligns in the [$\bar{1}$10] direction. On the other hand, antiferromagnetic Gd spins align in the axis parallel to the [$\bar{1}$10] direction with a slight tilting of an antiferromagnetic component, which is antiparallel to the applied field, from [1$\bar{1}$0] towards the direction of the applied field H. In this case, $(\chi_{Cu\perp}+\chi_{Gd\parallel})$ must be used instead of $(\chi_{Cu}+\chi_{Gd})$ in Eq. (2). Since $\chi_{Cu\perp}$ seems to be larger than $\chi_{Gd\parallel}$, the contribution of $\chi_{Cu\perp}$ would be dominant in this field range. The magnetization jump observed in the [$\bar{1}$10] direction at 1.8 kOe is considered to be a flop of antiferromagnetic Gd spins from a parallel to a perpendicular spin arrangement regarding the direction of the applied field. In this case, the critical field H_c for spin flopping of antiferromagnetically coupled Gd spins is given by

$$H_c=\sqrt{\frac{2K}{\chi_{Gd\perp}-\chi_{Gd\parallel}}}, \tag{3}$$

where K is the anisotropy constant and $\chi_{Gd\perp}$ and $\chi_{Gd\parallel}$ are perpendicular and parallel magnetic susceptibilities, respectively. In the geometry in which a magnetic field is applied to the [$\bar{1}$10] direction, the field-dependent term in Eq. (2) is given by $(\chi_{Cu\perp}+\chi_{Gd\perp})H$ at magnetic fields above 1.8 kOe. Therefore, since $(\chi_{Gd\perp}-\chi_{Gd\parallel})$ is obtained by subtracting $(\chi_{Cu\perp}+\chi_{Gd\parallel})$ from $(\chi_{Cu\perp}+\chi_{Gd\perp})$, the anisotropy constant K can be estimated using Eq. (3). Here $K=6.05\times10^3$ erg/cm^3 was obtained by using $H_c=1.8$ kOe, $(\chi_{Cu\perp}+\chi_{Gd\parallel})=6.49\times10^{-3}$ emu/cm^3, and $(\chi_{Cu\perp}+\chi_{Gd\perp})=1.02\times10^3$ emu/cm^3. On the other hand, a magnetization jump is observed at 2.7 kOe when a magnetic field is applied to the [100] direction. In this geometry, the field component in the [$\bar{1}$10] direction causes the spin flopping, and the component is given by $H_{110}=H\cos\theta$, where θ is the angle between H and the [$\bar{1}$10] direction. When $\theta=\pi/4$ rad and $H=2.7$ kOe

TABLE I. Irreducible representations and vector components of the base vectors for Cu($4a$) sites.

Irreducible representations	Vector components		
	x	y	z
$\Gamma_1(+\ +\ +)$	A	G	C
$\Gamma_2(+\ -\ +)$	F	C	G
$\Gamma_3(-\ +\ -)$	C	F	A
$\Gamma_4(-\ -\ +)$	G	A	F

were used, $H_{110}=1.9$ kOe was deduced. This value is consistent with the critical field H_c (=1.8 kOe) for the spin flopping observed in the $[\bar{1}10]$ direction. Moreover, this model is consistent with the angular dependence observed in the $M(\theta)$ at 3 K (Fig. 12). Since the ground state of Gd^{3+} is $^8S_{7/2}$ and, consequently, large one-ion magnetic anisotropy cannot be expected, the antiferromagnetic order in the Gd sublattice would be considerably affected by the applied magnetic field and the magnetism in the Cu sublattice.

The magnetic structure in $Gd_{1.85}Ce_{0.15}CuO_4$ crystals can be estimated by taking the crystal symmetry into account. When the four basis vectors of $\mathbf{F}=\mathbf{S}_1+\mathbf{S}_2+\mathbf{S}_3+\mathbf{S}_4$, $\mathbf{G}=\mathbf{S}_1-\mathbf{S}_2+\mathbf{S}_3-\mathbf{S}_4$, $\mathbf{C}=\mathbf{S}_1+\mathbf{S}_2-\mathbf{S}_3-\mathbf{S}_4$, and $\mathbf{A}=\mathbf{S}_1-\mathbf{S}_2-\mathbf{S}_3+\mathbf{S}_4$ are considered for the Cu($4a$) sites of *Bmab*, irreducible representations of these vectors are obtained following Bertaut's representation theory.[33] The irreducible representations of the basis vectors for Cu($4a$) sites are shown in Table I. Since the components of basis vectors in the same representation can be coupled, a canted spin structure is attained. In these representations, antiferromagnetically coupled sublattice moments must be parallel to the [110] direction in Γ_1, Γ_3, and Γ_4 and parallel to the [001] direction in Γ_2, and a spontaneous WF moment can be observed along the [110], $[\bar{1}10]$, and [001] directions in Γ_2, Γ_3, and Γ_4, respectively. According to the results of magnetic measurements mentioned above, Cu-sublattice moments are always parallel to the [110] direction regardless of the different magnetic phases, and a WF moment is parallel to the $[\bar{1}10]$ direction in phases I and III. Therefore, among the representations, Γ_3 is consistent with the magnetism in phases I and III, and Γ_1 is consistent with the magnetism of phase II at a low magnetic field. Possible spin configurations in these magnetic phases are shown in Fig. 15. Antiferromagnetically coupled sublattice moments of Gd are parallel to the $[\bar{1}10]$ direction at a low magnetic field at 3 K in phase I and paramagnetic at 6 and 20 K, respectively, in phase II and III. However, when a magnetic field with high intensity is applied to the $[\bar{1}10]$ direction, the antiferromagnetic sublattice moments of Gd flop and become parallel to the [110] direction in phase I, and the spin configuration of Cu ions in phase II transforms from Γ_1 to Γ_3 through a field-induced spin-reorientation transition, inducing a spontaneous WF moment of Cu spins along the $[\bar{1}10]$ direction. In the thermomagnetic curve shown in the inset of Fig. 6, a thermal hysteresis was observed at transitions A and B. Since the thermal hysteresis is a typical characteristic of the first-order phase transition, the phase transition between antiferromagnetic Γ_1 and weak-ferromagnetic Γ_3 phases appears to be a first-order phase transition. The isotropic exchange interaction between Cu and Gd ions is thought to play a key role in the spin reorientation at T_{SR}. When the spin moment of the Gd ion increases at low temperature and then the isotropic exchange interaction $\Sigma_{i\neq j}\tilde{J}_{ij}\mathbf{S}_j^{Cu}\cdot\mathbf{S}_j^{Gd}$ (or the interaction energy between Cu spins and H_i) is enhanced and exceeds the anisotropy energy of Cu ions at a specific temperature ($=T_{SR}$), the Cu spins undergo a spontaneous spin reorientation similar to that observed in the orthoferrites and orthochromites. Since Gd^{3+} is an *S*-state ion, the anisotropy energy of the Gd ion gives little contribution to the spin reorientation. It is important to the occurrence of the spin reorientation that the exchange coefficients $\tilde{D}$ and $\tilde{a}$ be comparable to the anisotropy constant *K*. This type of spin reorientation was observed for $DyFeO_3$.[34] $DyFeO_3$ shows a spin-reorientation transition from the low-temperature antiferromagnetic to the high-temperature weak-ferromagnetic spin configuration at about 30 K, and the magnetization shows a sharp increase. In the antiferromagnetic phase, no ferromagnetism is associated with the spin configuration of Fe^{3+} spins, and the spin moment of Dy^{3+} has therefore been considered to be paramagnetic. The abrupt (first-order) spin reorientation has been considered to be due to the isotropic interaction $\Sigma_{i\neq j}\tilde{J}_{ij}\mathbf{S}_i^{Fe}\cdot\mathbf{S}_j^{Dy}$ between the Fe^{3+} and Dy^{3+} sublattices.[25]

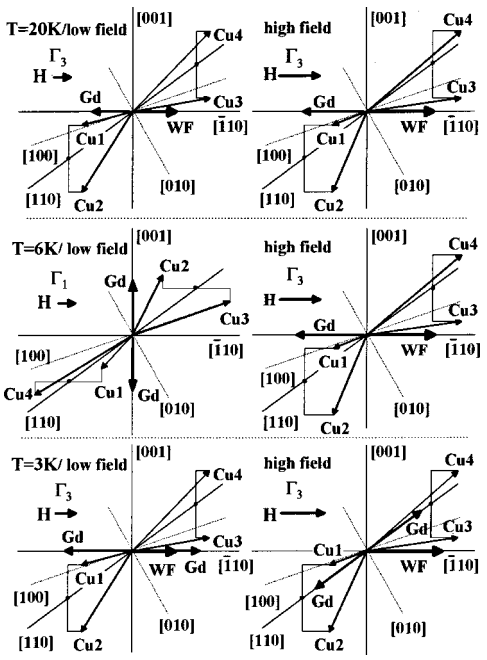

FIG. 15. Possible spin configurations in the various magnetic phases of $Gd_{1.85}Ce_{0.15}CuO_4$ crystal.

IV. CONCLUSION

The magnetic properties of $Sm_{1.85-x}Gd_xCe_{0.15}CuO_{4-\delta}$ and $Gd_{2-y}Ce_yCuO_{4-\delta}$ systems were investigated, and the interplay between superconductivity and magnetism was studied. All the transitions observed in the

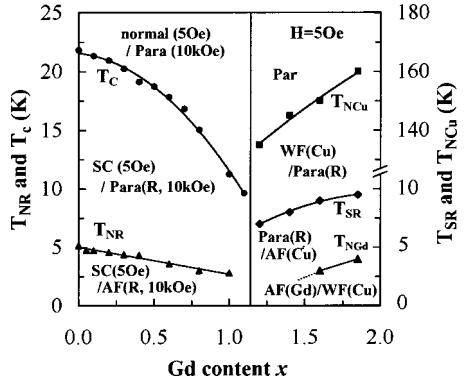

FIG. 16. Magnetic phase diagram for the $Sm_{1.85-x}Gd_xCe_{0.15}CuO_4$ system at temperatures below 180 K. Transition temperatures were determined under applied magnetic fields of 5 Oe and 10 kOe. T_c, T_{NR}, T_{NCu}, T_{NGd}, and T_{SR} are the superconducting transition temperature, the Néel temperature in the Sm, Cu, and Gd sublattices, and the spin-reorientation temperature, respectively. SC, WF, AF, and Para represent superconducting, weak-ferromagnetic, antiferromagnetic, and paramagnetic states, respectively, and (Cu) and (*R*) represent Cu and rare-earth sublattice, respectively.

$Sm_{1.85-x}Gd_xCe_{0.15}CuO_4$ system are summarized in Fig. 16 as a function of Gd content. A superconducting transition is observed for specimens with a Gd content of $0 \leqslant x \leqslant 1.1$. Sm spins have an antiferromagnetic order along the [001] direction below Néel temperature T_{NR} ($\sim$5 K for $x=0$), which is observed for specimens of $x \leqslant 1$ at high field intensity. The T_{NR} as well as the superconducting transition temperature T_c decreases with increasing Gd content and disappears for specimens of $x>1.1$. Successive magnetic transitions appear at about 3, 7, and 135 K as the Gd content increases over $x=1.1$. Although Cu spins have an antiferromagnetic order along the [110] direction among these transitions, a weak-ferromagnetic moment which is due to a canting of the Cu spins appears along the $[\bar{1}10]$ direction at temperatures of $T \leqslant 3$ K (phase I) and 7 K$\leqslant T \leqslant$135 K (phase III). The antiferromagnetic configuration of Cu spins at 3 K$<T<$7 K (phase II) is affected by the external field and changes into a weak-ferromagnetic spin configuration, which is the same structure as that in phase III, via field-induced spin reorientation. The transition at 7 K is a temperature-induced spin-reorientation transition between antiferromagnetic (phase II) and weak-ferromagnetic (phase III) spin configurations in the Cu sublattice. The reorientation temperature T_{SR}, which is observed at very low field intensity, shifts to higher temperatures with increasing x. On the other hand, the transition at 3 K is an antiferromagnetic transition in the Gd sublattice. The transition, which is characterized by Néel temperature T_{NGd} and is observed for $x>1.5$, shifts to higher temperatures with increasing Gd content. With the formation of an antiferromagnetic order in the Gd sublattice, Cu spins reorient from an antiferromagnetic ($T \geqslant T_{NGd}$) to a weak-ferromagnetic ($T \leqslant T_{NGd}$) configuration. Peaks at T_{NGd} and T_{SR} are sensitive to the magnetic field: they merge at about 2 kOe and disappear at a magnetic field of about 10 kOe.

The results of this study suggest that Gd substitution changes the magnetic structure of host material $Sm_{1.85}Ce_{0.15}CuO_4$ and suppresses superconductivity. The suppression of the superconductivity is attributed to the geometry of rare-earth and Cu spins. In $Sm_{1.85}Ce_{0.15}CuO_4$, antiferromagnetically coupled Sm spins are parallel to the [001] direction and perpendicular to the Cu spins, which couple antiferromagnetically in the *ab* plane, while, in $Gd_{1.85}Ce_{0.15}CuO_4$, both Gd and Cu spins are parallel to the *ab* plane. Since the exchange interaction between rare-earth and Cu spins in the same plane must be stronger than that of a perpendicular spin configuration, the fluctuation of Cu spins must be suppressed by the interaction, and the superconductivity of $Sm_{1.85}Ce_{0.15}CuO_4$ would thus be suppressed by the Gd substitution.

ACKNOWLEDGMENTS

We would like to thank Professor R. N. Shelton, Dr. J. Z. Liu, and P. Klavins for their helpful suggestions to this study. We are thankful for the electron diffraction analysis to H. Fujiki and H. Minagawa. The work done at Aoyama Gakuin University was supported by a Grant-in-Aid for Scientific Research from the Ministry of Education, Science, Sports and Culture, Japan, and a part of the work done at Aoyama Gakuin University was supported by a grant from The Research Institute of Aoyama Gakuin University. Part of the work performed at National Chung Hsing University was supported by the National Science Council of the Republic of China under Grant No. NSC 89-2112-M-005-006.

*Corresponding author. FAX:- 03-5384-6416. Electronic address: ynag@ee.aoyama.ac.jp

[1] Y. Tokura, H. Takagi, and S. Uchida, Nature (London) **337**, 345 (1989).

[2] S. Skanthakumar, H. Zhang, T. W. Clinton, W. H. Li, J. W. Lynn, Z. Fisk, and S. W. Cheong, Physica C **160**, 124 (1989).

[3] Y. Endoh, M. Matsuda, K. Yamada, K. Kakurai, Y. Hidaka, G. Shirane, and R. J. Birgeneau, Phys. Rev. B **40**, 7023 (1989).

[4] D. E. Cox, A. I. Goldman, M. A. Subramanian, J. Gopalakrishnan, and A. W. Sleight, Phys. Rev. B **40**, 6998 (1989).

[5] P. Allenspach, S. W. Cheong, A. Dommann, P. Fischer, Z. Fisk, A. Furrer, H. R. Ott, and B. Rupp, Z. Phys. B: Condens. Matter **77**, 185 (1989).

[6] S. Skanthakumar, H. Zhang, T. W. Clinton, I. W. Sumarlin, W. H. Li, J. W. Lynn, Z. Fisk, and S. W. Cheong, J. Appl. Phys. **67**, 4530 (1990).

[7] T. R. Thurston, M. Matsuda, K. Kakurai, K. Yamada, Y. Endoh, R. J. Birgeneau, P. M. Gehring, Y. Hidaka, M. A. Kastner, T. Murakami, and G. Shirane, Phys. Rev. Lett. **65**, 263 (1990).

[8] J. N. Lynn, I. W. Sumarlin, S. Skanthakumar, W. H. Li, R. N. Shelton, J. L. Peng, Z. Fisk, and S. W. Cheong, Phys. Rev. B **41**, 2569 (1990).

[9] S. Skanthakumar, J. W. Lynn, J. L. Peng, and Z. Y. Li, J. Appl. Phys. **69**, 4866 (1991).

[10] I. W. Sumarlin, S. Skanthakumar, J. W. Lynn, J. L. Peng, Z. Y. Li, W. Jiang, and R. L. Greene, Phys. Rev. Lett. **68**, 2228 (1992).

[11] S. Skanthakumar, J. W. Lynn, J. L. Peng, and Z. Y. Li, J. Magn. Magn. Mater. **104–107**, 519 (1992).
[12] T. Chattopadhyay, P. J. Brown, B. Roessli, A. A. Stepanov, S. N. Baliro, and D. I. Zhibunov, Phys. Rev. B **46**, 5731 (1992).
[13] M. B. Maple, N. Y. Ayoub, T. Bjornholm, E. A. Early, S. Ghamaty, B. W. Lee, J. T. Markert, J. J. Neumeier, and C. L. Seaman, Physica C **164**, 296 (1989).
[14] J. Akimitsu, H. Sawa, T. Kobayashi, H. Fujiki, and Y. Yamada, J. Phys. Soc. Jpn. **58**, 2646 (1989).
[15] T. Chattopadhyay, P. J. Brown, A. A. Stepanov, P. Wyder, J. Voiron, A. I. Zvyagin, S. N. Baliro, D. I. Zhibunov, and I. Zobkalo, Phys. Rev. B **44**, 9486 (1991).
[16] A. A. Stepanov, P. Wyder, T. Chattopadhyay, P. J. Brown, I. M. Vitebsky, A. Deville, B. Gaillard, S. N. Barilo, and D. I. Zhigunov, Phys. Rev. B **48**, 12 979 (1993).
[17] Y. Nagata, M. D. Lan, P. Klavins, and R. N. Shelton, Bull. Am. Phys. Soc. **36**, 668 (1991).
[18] Y. Nagata, T. Okamoto, N. Suzuki, T. Uchida, M. D. Lan, L. Zhang, P. Klavins, and R. N. Shelton, Physica C **185–189**, 1109 (1991).
[19] A. Butera, A. Caneiro, M. T. Causa, L. B. Steren, R. Zysler, M. Tovar, and S. B. Oseroff, Physica C **160**, 341 (1989).
[20] Y. Dalichaouch, B. W. Lee, C. L. Seaman, J. T. Markert, and M. B. Maple, Phys. Rev. Lett. **64**, 599 (1990).
[21] L. B. Steren, M. Tovar, and S. B. Oseroff, Phys. Rev. B **46**, 2874 (1992).
[22] J. D. Thompson, S. W. Cheong, S. E. Brown, Z. Fisk, S. B. Oseroff, M. Tovar, D. C. Vier, and S. Schultz, Phys. Rev. B **39**, 6660 (1989).
[23] S. B. Oseroff, D. Rao, F. Wright, M. Tovar, D. C. Vier, S. Schultz, J. D. Thompson, Z. Fisk, and S. W. Cheong, Solid State Commun. **70**, 1159 (1989).
[24] S. B. Oseroff, D. Rao, F. Wright, D. C. Vier, S. Schultz, J. D. Thompson, Z. Fisk, S. W. Cheong, M. F. Hundley, and M. Tovar, Phys. Rev. B **41**, 1934 (1990).
[25] T. Yamaguchi, J. Phys. Chem. Solids **35**, 479 (1974).
[26] T. Moriya, in *Magnetism*, edited by G. T. Rado and H. Suhl (Academic, New York, 1963), Vol. 1, p. 85.
[27] P. Galez, P. Schweiss, G. Collin, and R. Bellissent, J. Less-Common Met. **164–165**, 784 (1990).
[28] P. Adelmann, R. Ahrens, G. Czjzek, G. Roth, H. Schmidt, and C. Steileitner, Phys. Rev. B **46**, 3619 (1992).
[29] R. D. Zysler, M. Tover, C. Rettori, D. Rao, H. Shore, S. B. Oseroff, D. C. Vier, S. Schultz, Z. Fisk, and S. W. Cheong, Phys. Rev. B **44**, 9467 (1991).
[30] A. H. Cooke, D. M. Martin, and M. R. Wells, J. Phys. C **7**, 3133 (1974).
[31] C. L. Seaman, N. Y. Ayoub, T. Bjornholm, E. A. Early, S. Ghamaty, B. W. Lee, J. T. Markert, J. J. Neumeier, P. K. Tsai, and M. B. Maple, Physica C **391–403**, 159 (1989).
[32] G. H. Hwang, J. H. Shieh, J. C. Ho, and H. C. Ku, Physica C **201**, 171 (1992).
[33] E. F. Bertaut, in *Magnetism*, edited by G. T. Rado and H. Suhl (Academic, New York, 1963), Vol. 3, p. 149.
[34] M. Belakhovsky, M. Bogé, J. Chappert, and J. Sivardière, Solid State Commun. **20**, 473 (1976).